

Accessibility Control on Copper(II) Complexes in Mesostructured Porous Silica Obtained by Direct Synthesis using Bidentate Organosilane Ligands

Wen-Juan Zhou,^{†,‡} Belén Albela,[†] Pascal Perriat,[§] Ming-Yuan He,[‡] and Laurent Bonneviot^{*†}

[†]Laboratoire de Chimie, Ecole Normale Supérieure de Lyon UMR-CNRS 5182, Université de Lyon, 46 Allée d'Italie, 69364 Lyon Cedex 07, France, [‡]Shanghai Key Laboratory of Green Chemistry and Chemical Process, East China Normal University, No. 3663, North Zhongshan Road, 200062, Shanghai, China, and [§]Laboratoire MATEIS, INSA de Lyon, Bâtiment Blaise Pascal, 7 Avenue Jean Capelle, Lyon, France

Received April 7, 2010. Revised Manuscript Received June 18, 2010

The accessibility of metal(II) complexes in 2D hexagonal mesostructured porous silicas obtained by direct synthesis is controlled using an appropriate organosilane ligand. This is exemplified here using copper(II) as a transition metal probe and a neutral or negatively charged ligand: N-(2-aminoethyl)-3-aminopropyltrimethoxysilane, **L_A**, and N-salicylaldimine-propylamine-trimethoxysilane, **L_B**, respectively. **L_A** leads to inaccessible complexes located into the pore wall and called “embedded” sites here where silanolate groups from the siliceous network block the access to Cu(II) ions. By contrast, **L_B** generates accessible complexes, named “showing-on” sites here. The copper-containing silicas were synthesized with various metal molar ratios (M/SiO₂ = 0.5–3%) in basic media, with cetyltrimethylammonium *p*-toluenesulfonate (CTATos) as template and with sodium silicate solution as silicon source. A soft template extraction procedure has been developed to preserve the complex integrity of the showing-on copper sites during the treatment. The embedded copper(II) and nickel(II) sites were compared. Materials containing embedded, showing-on, and grafted sites were also compared with regard to pore size, surface polarity, and metal leaching. The material containing showing-on sites was found to be catalytically active for the hydroxylation of phenol into catechol and hydroquinone. Both textural and structural properties of the material and the copper sites were investigated using XRD, TEM, N₂ sorption isotherms, TGA, FT-IR, UV–visible, and EPR spectroscopies.

Introduction

The development of various and eventually “orthogonal” strategies to synthesize functional solids are important particularly to combine different types of active sites with various properties. For instance, combining conductivity and magnetism or superparamagnetism and fluorescence is crucial in diagnosis and therapy.^{1–5} In catalysis, combining antagonist sites such as acid and base functions can lead to synergic effects as in enzymes.^{6–8} In that context, mesostructured porous silicas⁹ are good candidates to develop tunable multifunctional materials. Conveniently, their internal surface presents a high silanol density useful for grafting various specific functions. For example, dual grafting of molecular “stirrers” and “gates” has been performed in a MCM-41 solid.¹⁰ Alternatively, organic functions can be

directly introduced in the sol–gel synthesis of the mesostructured silica according to direct synthesis and eventually synthesis route.^{11–15} These latter approaches lead to species located in the framework of the pore wall by contrast to surface species obtained by grafting. Both techniques may be combined to generate multifunctional mesostructured systems. For a direct synthesis, precursors with the organic moiety linked to at least two condensable alkyltrialkoxysiloxane arms are required; then, periodic mesostructured organosilicas materials (PMOs) may be obtained following a sol–gel route in the presence of templating surfactants.^{16–19} The latter technique is rather successful for small organic moieties but seems up to now limited for bulky ones such as transition metal complexes. The present study focuses on such direct incorporation of transition metal ions adding an accessibility control of the coordination to external molecules.

Indeed, because of their large size, the incorporation of metal complexes in the pore wall of ordered mesoporous silicas using a direct synthesis route remains challenging: ethylenediamine complexes with Cu(II) in HSM silicas¹¹ and cyclam complexes with Cu(II) and Co(II) in SBA-15^{13,14} both in neutral synthetic

*Corresponding author. Laurent. Bonneviot, fax: +33 472 72 88 60; tel: +33 472 72 83 91; e-mail: laurent.bonneviot@ens-lyon.fr.

(1) Tsai, C. P.; Hung, Y.; Chou, Y. H.; Huang, D. M.; Hsiao, J. K.; Chang, C.; Chen, Y. C.; Mou, C. Y. *Small* **2008**, *4*, 186.

(2) Kim, J.; Kim, H. S.; Lee, N.; Kim, T.; Kim, H.; Yu, T.; Song, I. C.; Moon, W. K.; Hyeon, T. *Angew. Chem-Int. Edit.* **2008**, *47*, 8438.

(3) Julian-Lopez, B.; Boissiere, C.; Chaneac, C.; Grosso, D.; Vasseur, S.; Miraux, S.; Duguet, E.; Sanchez, C. *J. Mater. Chem.* **2007**, *17*, 1563.

(4) Cornia, A.; Costantino, A. F.; Zoppi, L.; Caneschi, A.; Gatteschi, D.; Mannini, M.; Sessoli, R. *Single-Mol. Magn. Relat. Phenom.* **2006**, *122*, 133–161.

(5) Lu, A. H.; Schüth, F. *Adv. Mater.* **2006**, *18*, 1793.

(6) Anan, A.; Sharma, K. K.; Asefa, T. *J. Mol. Catal. A: Chem.* **2008**, *288*, 1.

(7) Gelman, F.; Blum, J.; Schumann, H.; Avnir, D. *J. Sol-Gel Sci. Technol.* **2003**, *26*, 43.

(8) Zhang, F.; Liu, G. H.; He, W. H.; Yin, H.; Yang, X. S.; Li, H.; Zhu, J.; Li, H. X.; Lu, Y. F. *Adv. Funct. Mater.* **2008**, *18*, 3590.

(9) Beck, J. S.; Vartuli, J. C.; Roth, W. J.; Leonowicz, M. E.; Kresge, C. T.; Schmitt, K. D.; Chu, C. T. W.; Olson, D. H.; Sheppard, E. W.; McCullen, S. B.; Higgins, J. B.; Schlenker, J. L. *J. Am. Chem. Soc.* **1992**, *114*, 10834.

(10) Zhu, Y. C.; Fujiwara, M. *Angew. Chem., Int. Ed.* **2007**, *46*, 2241.

(11) Karakassides, M. A.; Fournaris, K. G.; Travlos, A.; Petridis, D. *Adv. Mater.* **1998**, *10*, 483.

(12) Karakassides, M. A.; Bourlinos, A.; Petridis, D.; Coche-Guerente, L.; Labbe, P. *J. Mater. Chem.* **2000**, *10*, 403.

(13) Corriu, R. J. P.; Mehdi, A.; Reyé, C.; Thieuleux, C. *Chem. Commun.* **2003**, 1564.

(14) Corriu, R. J. P.; Mehdi, A.; Reyé, C.; Thieuleux, C. *Chem. Commun.* **2002**, 1382.

(15) Corriu, R. J. P.; Mehdi, A.; Reyé, C.; Thieuleux, C. *New J. Chem.* **2003**, *27*, 905.

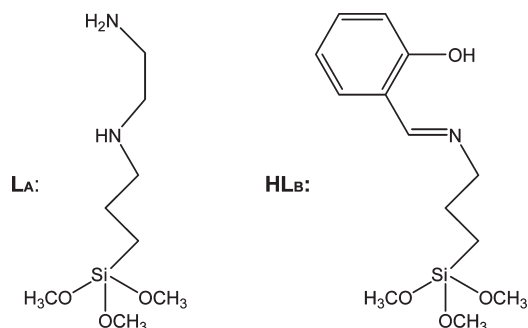
(16) Inagaki, S. *Nanotechnol. Mesostruct. Mater.* **2003**, *146*, 1.

(17) Inagaki, S.; Guan, S.; Fukushima, Y.; Ohsuna, T.; Terasaki, O. *J. Am. Chem. Soc.* **1999**, *121*, 9611.

(18) Hunks, W. J.; Ozin, G. A. *J. Mater. Chem.* **2005**, *15*, 3716.

(19) Asefa, T.; MacLachlan, M. J.; Coombs, N.; Ozin, G. A. *Nature* **1999**, *402*, 867.

Scheme 1. Organosilane Ligands L_A and HL_B Used for Incorporation of Copper or Nickel in the Mesoporous Materials



conditions, again ethylenediamine copper(II) complexes and also vanadyl Schiff base complexes in MCM-41 using a basic route^{12,20} and, also, phosphinorhodium(I) complexes in SBA-3 using an acidic route.²¹ In all the cases, the metal ion is complexed by a single tetradentate macrocycle with four polycondensable groups, by a single tetradentate ligand with two polycondensable groups, or by three monodentate organosilane ligands, respectively. Bidentate ligands with one organosilane polycondensable arm can be used as long as there are at least two such ligands per metal ion.^{11,12,22} The metal ion concentration has to remain relatively low (< 5%) mainly to preserve the mesostructure; therefore, they may not be regarded as PMO materials, despite the high C/Si molar ratio that can be reached (ca. 20%). Furthermore, the pH, the temperature, and the choice of ligand are key parameters to maintain the complex integrity and to obtain a control on their location in the final material.^{12,21,22} However, it is not clear yet what are the key parameters that control the metal accessibility required for eventual adsorption or catalytic properties. To our knowledge, there is no other work reporting specifically on that matter.

Using the basic synthesis route, we have previously reported that nickel(II) complexed with the bidentated neutral ligand, L_A (see abstract and Scheme 1), leads to framework complexes that are not accessible to external molecules and are resistant to acid leaching despite the very small pore wall thickness (~1 nm) of the mesostructured host matrix.²² The coordination of nickel(II) is characterized by two bidentate L_A ligands and, in addition, two silanolate groups that are locking the metal accessibility. This observation prompted us to find a way to avoid such a coordination blockage by moving from a neutral bidentate ligand to a negatively charged ligand that might compete favorably with the blocking effect of the silanolate ligands. From the demonstration, this ligand had to be structurally related to L_A .

The organosilane ligand of choice is the hemisalen (salicylaldimine), HL_B (see Abstract and Scheme 1), that produces well-characterized neutral $M(L_B)_2$ complexes with $M = Co^{2+}$, Cu^{2+} , Ni^{2+} .^{23–27} Besides, such metal complexes are very interesting per se, since they are known to afford selective catalytic oxidation reactions.²⁶ Here, Cu(II) is preferred owing to its highly

structure sensitive electron paramagnetic resonance (EPR) response.²⁷ For comparison, mesoporous materials possessing framework Cu(II) and Ni(II) species using L_A were prepared using a similar method as before except for the extraction of the surfactant cetyltrimethylammonium, CTA^+ . Previously, the displacement of CTA^+ and the capping of the silanol by trimethylsilyl using a silylation agent was performed to avoid the collapse of the silica mesostructure (reminding that it is synthesized at low temperature ~60 °C).^{21,22} Here, the new extraction method consists merely of a soft acidic treatment using 1 mol equiv of HCl vs the surfactant that allows better control on the complex built from L_B^- . In complement, a metal free and MCM-41 (LUS) where $[Ni(L_A)_2]^{2+}$ complexes have been postgrafted were used also for comparison. Note that the new extraction procedure has been also applied for the nickel-containing material generating here an original set of samples that are not silylated (no silanol capping in the channel) in comparison to our previous study.²² The structure and the texture of the materials have been investigated using XRD, N_2 sorption isotherms, and TEM techniques. The nature and the quantity of the loaded species have been determined from FT-IR spectroscopy, elemental analysis (EA), ICP-MS, and TGA measurements. Furthermore, the metal displacement upon acidic treatment has been tested in both types of materials and monitored using EPR spectroscopy. Finally, the catalytic activity on the hydroxylation of phenol into diphenols (catechol and hydroquinone) has been also studied.

Experimental Section

1. Materials. Copper(II) acetate trihydrate (99%, Acros), copper(II) nitrate pentahydrate (99%, Acros), nickel(II) nitrate hexahydrate (99%, Acros), sodium hydroxide (Acros), 3-amino-propyl-trimethoxysilane (95%, Acros), salicylaldehyde (98%, Avocado), *N*-(2-aminoethyl)-3-aminopropyltrimethoxysilane (L_A ; 97%, Acros), Ludox HS-40 (40% SiO_2 ; Aldrich), hexadecyltrimethylammonium-*p*-toluene-sulfonate, (CTATos; > 99% Merck), HCl (1 mol·L⁻¹, Acros), ethanol (96%, Elvetec; anhydrous, Carlo Erba, HPLC quality), potassium phosphate monobasic (99%, Acros), disodium hydrogen phosphate (anhydrous, > 99%, Merck), phenol (≥99%, Sigma-Aldrich), catechol (99%, Acros), and hydroquinone (≥99%, Fluka) were used as received. The sodium silicate solution was prepared as follows: Ludox HS-40 (187 mL) was added to sodium hydroxide (32 g) in deionized water (800 mL) and stirred at 40 °C until clear.

2. Synthesis. **2.1. Direct Synthesis of Materials DS-Ni L_A and DS-Cu L_A .** A sodium silicate solution (40 mL) was stirred at 60 °C for 1 h. A second solution of hexadecyltrimethylammonium *p*-toluenesulfonate (CTATos, 1.8 g) in deionized water (50 mL) was stirred during 1 h at 60 °C. A solution containing 0.28 mmol of $[Ni(L_A)_2](NO_3)_2$ ($M/SiO_2 = 0.3\%$, $L_A = N$ -(2-aminoethyl)-3-aminopropyltrimethoxysilane) or 0.84 mmol of $[Cu(L_A)_2](NO_3)_2$ ($M/SiO_2 = 1\%$) was added to the first solution and stirred until homogeneous. The solutions remain clear up to this point. By contrast, a rapid condensation of the silica takes place when this solution is added dropwise during 20 min at 60 °C to the second solution containing the templating ammonium. The colloidal solutions formed were further stirred at 60 °C for 24 h. After filtration and washing with deionized water (200–300 mL), the as-made solids were dried in the oven at 60 °C for 2 days, obtaining 2.1 g of DS-Ni L_A and 3.0 g of DS-Cu L_A , respectively. EA for DS-Ni L_A : C (30.41%), N (2.23%), Ni (0.61%), weight loss at 1000 °C (46.59%), and DS-Cu L_A : C (31.16%), N (3.22%), Cu (1.67%), weight loss at 1000 °C (51.07%).

2.2. Synthesis of HL_B Ligand. A two-neck round-bottom flask with a condenser was first vacuumed at room temperature and then filled with argon, and the same procedure was repeated three times. Salicylaldehyde (0.57 mL, 5 mmol) and anhydrous ethanol (22 mL) were introduced into the flask.

(20) Baleizao, C.; Gigante, B.; Garcia, H.; Corma, A. *J. Catal.* **2003**, *215*, 199.
(21) Dufaud, V.; Beauchesne, F.; Bonneviot, L. *Angew. Chem., Int. Ed.* **2005**, *44*, 3475.

(22) Zhou, W. J.; Albela, B.; Ou, M.; Perriat, P.; He, M. Y.; Bonneviot, L. *J. Mater. Chem.* **2009**, *19*, 7308.

(23) Chandran, D.; Kwak, C. H.; Ha, C. S.; Kim, I. *Catal. Today* **2008**, *131*, 505.

(24) Chakraborty, J.; Nandi, M.; Mayer-Figge, H.; Sheldrick, W. S.; Sorace, L.; Bhaumik, A.; Banerjee, P. *Eur. J. Inorg. Chem.* **2007**, 5033.

(25) Luo, Y.; Lin, J. *Microporous Mesoporous Mater.* **2005**, *86*, 23.

(26) Murphy, E. F.; Schmid, L.; Burgi, T.; Maciejewski, M.; Baiker, A.; Gunther, D.; Schneider, M. *Chem. Mater.* **2001**, *13*, 1296.

(27) Murphy, E. F.; Ferri, D.; Baiker, M.; Van Doorslaer, S.; Schweiger, A. *Inorg. Chem.* **2003**, *42*, 2559.

3-Aminopropyltrimethoxysilane (0.90 mL, 5 mmol) was then added dropwise. The resulting mixture was stirred under reflux in the argon atmosphere for 6 h. The obtained yellow product was analyzed by ^1H NMR (300 MHz, CDCl_3): δ 0.76 (t, 2H, $J = 105$ 8.30 Hz), 1.89 (tt, 2H, $J = 8.20, 6.75$ Hz), 3.63 (t, 2H), 3.64 (s, 9H), 6.92 (t, 1H, $J = 7.49$ Hz), 7.01 (d, 1H, $J = 8.20$), 7.30 (dd, 1H, $J = 7.50$ Hz), 7.37 (d, 1H, $J = 7.46$ Hz), 8.40 (s, 1H). It was found impossible to crystallize this compound. Since the reaction was quantitative, there were negligible quantities of reactant detected on the NMR signal and the reaction mixture was used directly as a source for the synthesis of the solid.

2.3. Direct Synthesis of DS-CuL_B Materials. The above mixture was evaporated at 40 °C under vacuum, and the volume was reduced to 10 mL. Then, an ethanol solution (40 mL) of copper acetate monohydrate (0.479 g, 2.4 mmol) was added dropwise. The mixture was stirred under reflux in argon atmosphere for 2 h obtaining a solution (48.5 mL) containing the CuL_B complexes (no hydrolysis was observed despite the presence of water in the solid copper salt). Then, 1.7, 3.4, or 8.5 mL of this solution ($n\text{Cu} = 0.084, 0.17, 0.42$ mmol, $\text{M}/\text{SiO}_2 = 0.1\%, 0.2\%, 0.5\%$, respectively) were used to prepare materials DS-CuL_B, series using the same experimental procedure as for materials DS-NiL_A and DS-CuL_A. After washing with water and drying at 60 °C, about 2.8 g of solid was obtained in all cases. EA: C (33.3%), N (1.97%), Cu (0.24%), weight loss at 1000 °C (51.58%); C (32.09%), N (1.79%), Cu (0.35%), weight loss at 1000 °C (53.27%); C (31.94%), N (2.17%), Cu (0.94%), weight loss at 1000 °C (46.59%), respectively.

2.4. Direct Synthesis of Metal-Free Reference DS Material. A metal-free silica DS was prepared with similar conditions than materials DS-NiL_A and DS-CuL_A. EA: C (35.0%), H (7.4%), N (2.0%), weight loss at 1000 °C (58.1%). It is basically the low-temperature synthesis version of LUS usually autoclaved at 130 °C (vide infra).^{28,29}

2.5. Template Extraction. The solid (0.4 g, DS-NiL_A, DS-CuL_A or DS-CuL_B, and DS) was added into a two-neck round-bottom flask with a condenser. Then, technical ethanol (96%, 25 mL) and HCl (1 mol·L⁻¹, 0.54 mL, $n\text{HCl}:n\text{CTA}^+ = 1:1$) were added. The mixture was stirred at 40 °C for 1 h. The obtained solid was finally washed with technical ethanol (50 mL × 4) and acetone (50 mL × 2). The solids, DS-NiL_A-E (0.24 g), DS-CuL_A-E (0.25 g), DS-CuL_B-E (ca. 0.22 g), and DS-E (0.25 g) were respectively obtained. EA for DS-NiL_A-E: C (2.43%), N (1.01%), Ni (0.88%), weight loss at 1000 °C (13.37%); DS-CuL_A-E: C (5.97%), N (2.60%), Cu (2.50%), weight loss at 1000 °C (16.30%); DS-CuL_B-E with the smallest Cu/Si ratio: C (3.20%), N (0.21%), Cu (0.31%), weight loss at 1000 °C (89.62%); with the intermediate Cu/Si ratio: C (7.95%), N (1.74%), Cu (0.52%), weight loss at 1000 °C (83.49%); with the highest Cu/Si ratio: C (4.34%), N (0.56%), Cl (0.04%), Cu (1.06%), weight loss at 1000 °C (19.56%); DS-E: C (12.4%), H (3.6%), N (0.1%), weight loss at 1000 °C (12.8%).

2.6. Postsynthesis of Material PS-NiL_A. Material PS-NiL_A was synthesized starting from a 2D hexagonal silica prepared at 130 °C called LUS.^{29,30} The “molecular stencil patterning” (MSP) technique was used to homogeneously distribute the grafted

complexes, using trimethylsilyl functions (TMS) to separate each complex one from another.^{22,31,32}

2.6.1. Synthesis of Standard Metal Free 2D Hexagonal Mesoporous Silica PS. The synthesis was processed as for material DS replacing the 24 h stirring at 60 °C by autoclaving at 130 °C for 20 h. Six grams of LUS was obtained and designated here as PS to simplify the notation.²⁹ EA: C (32.7%), H (6.6%), N (2.0%), weight loss at 1000 °C (48.4%). PS-E was obtained after extraction of the template following the same protocol as for DS-E (see above).

2.6.2. Partial Template Extraction of PS. PS (10 g) was placed in a round-bottom flask, and then ethanol (400 mL, 96%) and hydrochloric acid 1 mol·L⁻¹ (6.8 mL, 1.1 equiv) were added. The mixture was stirred at 40 °C for 1 h. After filtration and washing with ethanol (100 mL × 2) and acetone (50 mL × 2), the solid was dried at 80 °C for 20 h. Material PS-PE (7.1 g) was obtained.

2.6.3. Partial Silylation of PS-PE. PS-PE (6.8 g) was added into a round-bottom three-neck flask, and then dried at 130 °C for 1 h under argon flow and during 2 h under vacuum. Cyclohexane (170 mL) and HMDSA (30 mL) were added under argon. The mixture was refluxed for 18 h. The obtained solid was finally washed with cyclohexane (2 × 30 mL), ethanol (2 × 60 mL), and acetone (2 × 60 mL) and then dried at 80 °C for 18 h. This sequence of steps was repeated twice. Partially silylated material PS-PES (7.1 g) was obtained. EA: C (19.7%), H (4.37%), N (0.7%), weight loss at 1000 °C (22.6%).

2.6.4. Extraction of Remaining Surfactant of PS-PES. PS-PES (2 g) was placed in a round flask, and then ethanol (86 mL, 96%) and hydrochloric acid (1.28 mL, 1 equiv, 1 mol·L⁻¹) were added. The mixture was stirred at 40 °C for 1 h. After filtration and washing with ethanol (50 mL) and acetone (50 mL), the obtained solid was dried at 80 °C for 20 h. The same procedure was repeated. Finally, material PS-PESE (1.4 g) was obtained. EA: C (7.8%), H (2.4%), N (<0.1%), weight loss at 1000 °C (10.7%).

2.6.5. Synthesis of Material PS-NiL_A. PS-PESE (0.5 g) was dried at 130 °C under argon flow during 1 h, and then evacuated under vacuum at 130 °C during 2 h. A solution of Ni(II) nitrate (0.28 mmol) and L_A ligand ($n\text{L}_A/n\text{Ni} = 2$) in 2 mL anhydrous ethanol was added together with 40 mL of toluene. The resulting mixture was stirred at 60 °C for 18 h under argon. After filtration, the obtained solid was washed with toluene (50 mL) and ethanol (25 mL), and then dried at 60 °C, obtaining 0.56 g of material PS-NiL_A. EA: C (12.1%), H (3.0%), N (3.5%), Ni (2.5%), weight loss at 1000 °C (19.3%).

2.7. Metal Extraction. The solid DS-NiL_A-E, DS-CuL_A-E, or DS-CuL_B-E (0.4 g) was added into a flask with a condenser. Then, ethanol (25 mL) and HCl (1 mol·L⁻¹, 0.5 mL, $n\text{HCl}:n\text{metal} = 8, 3, \text{ and } 8$, respectively) were added. The mixture was stirred at 40 °C for 1 h. After filtration and washing with technical ethanol (50 mL × 4) and acetone (50 mL × 2), the solids were dried at 60 °C for one day. Materials DS-NiL_A-H, DS-CuL_A-H, and DS-CuL_B-H (ca. 0.24 g) were obtained. For PS-NiL_A, the same process was employed (HCl 1 mol·L⁻¹, $n\text{HCl}:n\text{metal} = 9$) obtaining material PS-NiL_A-H.

2.8. Catalytic Test. Phenol hydroxylation experiments were performed at 80 °C for 2 h using a 50 mL two-neck round-bottom flask with a condenser. In a standard run, phenol (0.1 g, 1.1 mmol), catalyst (molar ratio Cu:phenol = 1:130), buffer solution pH = 6 (7 mL) and H₂O₂ (50% aqueous) were added in this order. The phenol and the products, catechol (CAT) and hydroquinone (HQ), were analyzed by HPLC.

3. Analytical Techniques. XRD: low-angle X-ray powder diffraction experiments have been carried out using a Bruker (Siemens) D5005 diffractometer using Cu K monochromatic radiation. IR: infrared spectra were recorded from KBr pellets using a Mattson 3000 IR-TF spectrometer. UV–visible: liquid UV–visible spectra were recorded using a Vector 550 Bruker

(28) Bonneviot, L.; Morin, M.; Badiei, A. Patent WO 01/55031 A 1 2001. this patent relates the use of CTATos as a surfactant where the presence of tosylate instead of inorganic anions reported in the other patent literature allows to produce an hexagonal mesostructured silica of high stability with much lower surfactant concentration. Then, the yield in surfactant is nearly 100% (no foam during washing). Incidentally, the CTA Tosylate salt is a cheaper surfactant source than the chloride or bromide analogue.

(29) Reinert, P.; Graillat, C.; Spitz, R.; Bonneviot, L. Proc. 3rd Int. Mesostructured Mat. Symp., Ryoo, R., Park, S., Eds. *Stud. Surf. Sci. Catal.*, **2003**, *146*, 439.

(30) Bonneviot, L.; Badiei, A.; Crowther, N. Patent WO 02216267 2002.

(31) Calmettes, S.; Albela, B.; Hamelin, O.; Ménage, S.; Miomandre, F.; Bonneviot, L. *New J. Chem.* **2008**, *32*, 727.

(32) Abry, S.; Thibon, A.; Albela, B.; Delichere, P.; Banse, F.; Bonneviot, L. *New J. Chem.* **2009**, *33*, 484.

spectrometer; solid diffuse reflectance UV–visible spectra were recorded from aluminum cells with Suprasil 300 quartz windows, using a PerkinElmer Lambda 950 and PE Winlab software. Nitrogen sorption isotherms at 77 K were determined with a volume device Micromeritics ASAP 2010 M on solids that were dried at 80 °C under vacuum overnight. TGA measurements were collected from Al₂O₃ crucibles on a DTA-TG Netzsch STA 409 PC/PG instrument, under air (30 mL/min), with a 25–1000 °C (10 °C/min) temperature increase. The silicon content was systematically measured from the residual mass at 1000 °C assuming that C, H, and N were all removed. This was cross-checked by elemental analysis on several samples with or without metal. In the presence of metal, a correction was performed assuming the formation of Cu₂O remaining at 1000 °C. Finally, the silicon coming from the organosilane was neglected when, as in most of the cases, it accounted for less than 4%.^{21,22,31,32,36,48} pH-meter (Meterlab pHM210) was calibrated in aqueous solution, so that the pH measured for the EtOH–H₂O is only indicative. EPR spectra were recorded using a Bruker Elexsys e500 X-band (9.4 GHz) spectrometer with a standard cavity. Quantification of Cu(II) species was performed using crystals of CuSO₄·5H₂O as calibration reference. TEM: imaging and analytical studies were performed on a JEOL 2010F microscope equipped with a field emission gun and operating at 200 kV. EDX (energy dispersive X-ray analysis) was performed with the help of a dispersive X-ray system (INCA-Oxford equipment) with a detector having a polymer ultrathin window. HPLC analyses were performed on a LC/MS Agilent 1100SLT. The working conditions are the following: column, ZORBAX-SB-C18 of dimension 4.6 mm × 250 mm; protect, 5 μm; loop size, 8 μL; temperature of the column, room temperature; UV detector, 245 and 280 nm; mobile phase, water (10 mmol/L formic acid, 60%) and acetonitrile (40%); flow rate, 0.2 mL/min.

Results and Discussion

1. Synthesis of the Materials. Five materials have been synthesized at 60 °C using direct synthesis (DS): **DS-NiL_A** and **DS-CuL_A**, with L_A ligand and starting from Ni(NO₃)₂ or Cu(NO₃)₂, respectively, and three **DS-CuL_B** materials with HL_B and various copper loading starting from Cu(AcO)₂. In all cases, the complex precursor was polycondensed in basic conditions with sodium silicate in the presence of hexadecyltrimethylammonium *p*-toluenesulfonate (CTATos) in water. For complexation with HL_B, the acetate counterion was preferred over nitrate to avoid acidity and hydrolysis of the imine bond of the ligand (vide infra).^{34,35} In all the materials, the initial molar L/M ratio was fixed at 2, according to previous studies with the Ni–L_A system, showing that these conditions yield mainly [Ni(L_A)₂]²⁺ species, whereas other ratios gave a mixture of complexes or/and free ligand.²²

The M/Si molar ratio in the mother gel was 0.3% and 1.0% for **DS-NiL_A** and **DS-CuL_A** and 0.1%, 0.2%, and 0.5% in the **DS-3CuL_B** series. The actual metal content was 1.2% and 3.2% for the ML_A series and 0.5%, 0.7%, and 1.6% for the CuL_B series, respectively (Supporting Information Table S1 and Experimental section). The **DS-CuL_B** series was designed to test the effect of the metal loading with ligand L_B. For the sake of simplification, **DS-CuL_B** refers to as the highest copper loaded material of the series otherwise stated. Note that the M/Si molar ratio in the solid is much higher than in the mother gel. Indeed, the yield of silicon was low, only ~30% for **DS-CuL_A** and **DS-CuL_B**, as for the

copper free reference, **DS**, whereas the yield of copper was nearly total (Table S2). In the case of the Ni-containing material, **DS-NiL_A**, both silicon and metal yields were lower, i.e., ~20% and ~80%, respectively. This is consistent with a higher rate of hydrolysis for the metalated alkoxyloxane than that of the silicate oligomers.²²

The metal-free material, **DS**-, was prepared in the very same conditions as the above-described metal-containing materials. The postgrafted material, **PS-NiL_A**, with the metal complexes located inside the pores, was prepared also with an L/M molar ratio equal to 2. The latter was synthesized using the so-called molecular stencil patterning (MSP) approach, which allows homogeneous distribution of a function on the internal surface of the pore of a 2D hexagonal mesostructured porous silica in basic conditions.^{22,31,32} Accordingly, starting from an as-made silica, **PS**, a controlled amount of the templating agent CTA⁺ is removed to lead to the partially extracted material **PS-PE**. Then, a silylation step with hexamethyldisilazane (HMDSA) is performed without displacement of the remaining CTA⁺ molecules to afford the partially extracted and silylated material **PS-PES**. After removal of the remaining CTA⁺ moieties, which play the role of stencil, the material **PS-PESE** is obtained. The latter undergoes the grafting of the metal complexes [M(L_A)₂]²⁺, yielding the postgrafted material **PS-NiL_A**.

The extraction of the template is a key point, since it should neither affect the coordination state of the metal nor provoke any metal leaching. A mere extraction of the templating agent may be obtained from either an acidic or nearly neutral treatment using HCl or NH₄AcO, respectively. Other extraction routes were investigated allowing concomitantly the capping of some of the silanol groups of the channel surface:²² direct silylating treatment using (i) chlorotrimethylsilane (TMSCl) with HCl evolution or (ii) a mixture of TMSCl and hexamethyldisilazane (HMDSA). The latter treatment was found to be the best to maintain the [Ni(L_A)₂] species in the framework position and preserve the hexagonal structure of the silica due to the more neutral media generated during the process.²² Nonetheless, these conditions were soft enough to retain copper in the **DS-CuL_B** series. The capping treatment was abandoned. Finally, it was found that a mere acid extraction using of only 1 equiv of HCl per surfactant was sufficient to neutralize the silanolate groups and to produce a nearly neutral solution that fully preserved the structure. This has been applied to generate the series of extracted solids, **DS-NiL_A-E**, **DS-CuL_A-E**, and **DS-CuL_B-E**. The latter present M/Si molar ratios of 0.010, 0.029, and 0.013 to be compared to 0.012, 0.032, and 0.016 for the mother materials **DS-NiL_A**, **DS-CuL_A**, and **DS-CuL_B**, respectively (Supporting Information Table S1). These figures indicate that the metal content remained nearly the same after such a soft treatment. For the grafted material **PS-NiL_A**, the M/Si molar ratio was 0.038.

The elemental analyses of the template extracted materials provide a N/M molar ratio of 4.8 for both **DS-NiL_A** and **DS-CuL_A**, indicating the presence of at least two L_A ligands per metal ion. However, in the postsynthesis material **PS-NiL_A**, the N/M value of 6.0 suggested the presence of two nitrate ions as counterions in addition of the two L_A.²² The presence of the latter ions was confirmed by IR spectroscopy. Finally, for **DS-CuL_B-E** a N/M molar ratio of 2.4 is consistent with the presence of at least two L_B ligands per metal ion in the material and the presence of non-coordinated L_B⁻ ligands due to a slight excess of ligand in the preparation.

2. Structure and Morphology of the Materials. All the materials are characterized by three XRD peaks assigned to (100), (200), and (210) reflections, consistent with a well-ordered

(33) Abry, S.; Albela, B.; Bonneviot, L. *C. R. Chim.* **2005**, *8*, 741.

(34) Fenton, D. E.; Westwood, G. P.; Bashall, A.; McPartlin, M.; Scowen, I. J. *J. Chem. Soc., Dalton Trans.* **1994**, 2213.

(35) Elias, H.; Hasserodt-Iaffero, C.; Hellriegel, L.; Schonherr, W.; Wannowius, K. *J. Inorg. Chem.* **1985**, *24*, 3192.

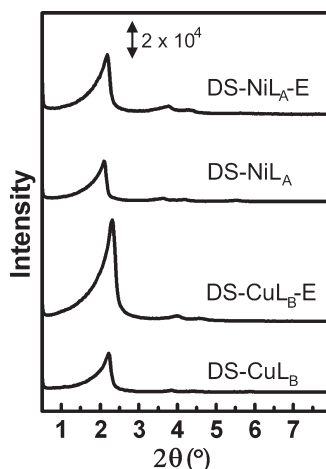


Figure 1. XRD patterns of materials DS-NiL_A-E, DS-NiL_A, DS-CuL_B-E, and DS-CuL_B.

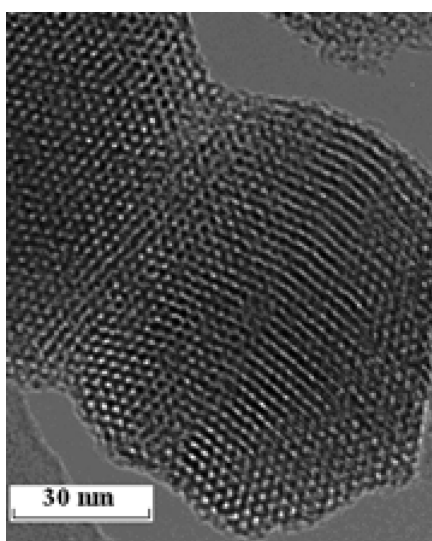


Figure 2. TEM image of DS-CuL_B-H (for Cu/Si = 0.5 mol %).

hexagonal array of channels like in MCM-41-type materials (Figure 1).^{9,32,36} Transmission electron microscopy (TEM) investigations also confirmed the highly ordered nature of the materials studied here as depicted in Figure 2 for DS-CuL_B-E. Note that the XRD pattern is about three times more intense for the template-extracted materials than for the as-made materials; indeed, this is expected when the channels are emptied without the loss of structure. In addition, template removal leads to structure shrinkage of about 5% according to a decrease of the a_0 parameter from 4.9, 5.1, and 4.6 in DS-NiL_A, DS-CuL_A, and DS-CuL_B down to 4.7, 4.8, and 4.4 nm in DS-NiL_A-E, DS-CuL_A-E, and DS-CuL_B-E, respectively. This is likely due to an increase of surface tension in the channel upon surfactant removal.

The nitrogen sorption isotherms performed on the extracted materials (Figure 3) are all of type IV according to the IUPAC classification.³⁷ The steep capillary condensation step at about 0.38 P/P_0 evidences a narrow pore size distribution.^{9,38} Strikingly,

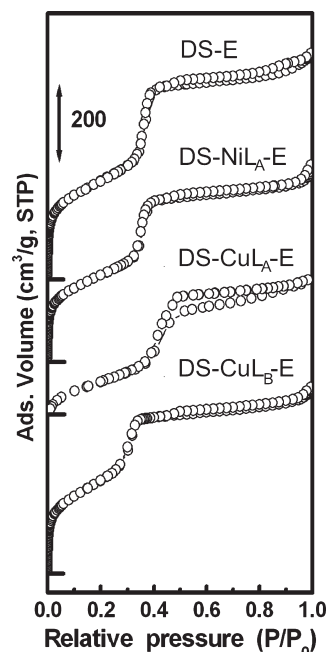


Figure 3. N₂ sorption isotherms at 77K of DS-E, DS-NiL_A-E, DS-CuL_A-E, and DS-CuL_B-E.

the pore diameter, ϕ_{BdB} , is the same within 0.1 nm, for materials DS-NiL_A-E and DS-CuL_A-E and for the metal-free reference DS-E, while it is smaller for DS-CuL_B-E (Table 1). The introduction of the metal complex in the DS series produces only a slight decrease of the specific surface area, S_{BET} , and the total porous volume, V_p . Nonetheless, the effect is more pronounced in a higher metal-loaded DS-CuL_A-E material than in DS-NiL_A-E. The horizontal hysteresis seen on the N₂ sorption isotherm for $P/P_0 > 0.4$ indicates the presence of defects found in a higher concentration for higher metal loadings.³⁹ Interestingly, the incorporation of the metal complex in the sol-gel synthesis does not affect the resulting pore wall thickness, W_t (Table 1). By contrast, the grafting of complexes such as Ni(L_A)₂ or amino-copper complexes in LUS, i.e., in both PS-NiL_A and PS-CuL_C,³² respectively, leads not only to a drastic decrease of pore volume, but also to a much thicker apparent wall thickness. This is consistent with an expected pore filling and a location of the complexes at the surface of the wall leading to an apparent thickening of ca. 0.5 nm.

These data strongly suggest that the metal complexes are located in the pore wall in the materials DS-NiL_A-E, DS-CuL_A-E, and DS-3CuL_B-E. By contrast, the presence of grafted species in PS-NiL_A obviously leads to an increase of the apparent pore thickness and to a decrease of the pore volume. Furthermore, the C parameter, which is calculated from the BET equation, is related to the surface polarity and provides complementary information on the surface modification. Indeed, the materials prepared with the metalated Ligand L_A are characterized by relatively high C values (~100) close to that of the metal-free material DS and consistent with little surface modification. By contrast, the organic grafted complexes in PS-NiL_A clearly decrease the surface polarity ($C = 34$). The material DS-CuL_B-E exhibits an intermediate value ($C = 83$) suggesting an intermediate situation in the materials using L_B.

In fact, the metal leaching test using an ethanolic solution of HCl in excess provides the most striking difference between

(36) Abry, S.; Lux, F.; Albela, B.; Artigas-Miquel, A.; Nicolas, S.; Jarry, B.; Perriat, P.; Lemerrier, G.; Bonneviot, L. *Chem. Mater.* **2009**, *21*, 2349.

(37) Sing, K. S. W.; Everett, D. H.; Haul, R. A. W.; Moscou, L.; Pierotti, R. A.; Rouquerol, J.; Siemieniewska, T. *Pure Appl. Chem.* **1985**, *57*, 603.

(38) Kresge, C. T.; Vartuli, J. C.; Roth, W. J.; Leonowicz, M. E. *Mesoporous Cryst. Relat. Nano-Struct. Mater.* **2004**, *148*, 53.

(39) Lin, H. P.; Wong, S. T.; Mou, C. Y.; Tang, C. Y. *J. Phys. Chem. B* **2000**, *104*, 8967.

Table 1. Textural Properties of Mesoporous Hybrid Materials from N₂ Sorption Isotherms at 77 K

material	S_{BET} (m^2g^{-1}) ± 50	V_p^a (cm^3g^{-1}) ± 0.02	ϕ_{BdB}^b ± 0.1	a_0^c (nm) ± 0.1	W_t^d (nm) ± 0.1	C^e
DS-E	1050	1.02	3.8	4.7	0.9	108
DS-NiL _A -E	910	0.85	3.8	4.7	0.9	106
DS-CuL _A -E	650	0.76	3.9	4.8	0.9	99
DS-CuL _B -E	1010	0.83	3.5	4.4	0.9	83
PS-NiL _A	860	0.46	3.4	4.8	1.4	34
PS-NiL _C ^f	590	0.45	3.3	4.7	1.4	-

^aTotal porous volume determined at $P/P_0 = 0.98$. ^b ϕ_{BdB} can be deduced by subtraction of 0.8 to the ϕ_{BdB} value. ^c $a_0 = 2d_{100}/\sqrt{3}$. ^d W_t , apparent wall thickness deduced from the BdB pore diameter and the d_{100} value in the XRD pattern ^e C parameter from BET equation. ^fCopper-amino complex grafted on a similar LUS support containing 1% wt Cu.³¹

materials. A neat discoloration was found for both DS-CuL_B-E and PS-NiL_A, leading to materials DS-3CuL_B-H and PS-NiL_A-H, respectively. By contrast, the color was maintained in DS-NiL_A-E and DSCuL_A-E. This is fully consistent with the chemical analysis showing a quantitative metal removal in the former cases (M/Si molar ratio of 0.004 and 0.003 for DS-CuL_B-H and PS-NiL_A-H, respectively, compared to 0.013 and 0.038 in the parent materials DS-CuL_B-E and PS-NiL_A, respectively, Supporting Information Table S1). The latter case (M/Si molar ratio of 0.007 and 0.026 for DS-1NiL_A-H and DS-CuL_A-H, respectively, compared to 0.010 and 0.029 in DS-NiL_A-E and DS-CuL_A-E, respectively, Supporting Information Table S1) indicates that the metal retention is about 70% and 90% with L_A, while a neat leaching of ca. 90% takes place with L_B.

3. Coordination of the Metal in the Materials. The coordination state of M-L_A systems was characterized by UV-visible and EPR techniques. The diffuse reflectance UV-visible spectrum of the solid DS-NiL_A presents two d-d bands at ~370 and ~600 nm, corresponding to the ν_3 and ν_2 transitions, respectively (Supporting Information Table S3).²²

The position of these two bands indicates the presence of two L_A ligands per Ni(II) ion, as in the initial aqueous solution.²² These bands were unchanged after extraction of the template (DS-NiL_A-E) and also after the metal leaching test (DS-NiL_A-H). This shows that the complex was not affected during these two different treatments. By contrast, the disappearance of the d-d bands in the visible region for the postsynthesis material, PS-NiL_A, after the metal leaching test is consistent with the quantitative Ni removal characterized above from chemical analyses (Supporting Information Table S1).

Material DS-CuL_A exhibits a single axial EPR signal for d⁹ Cu(II) cations with $g_{\parallel} = 2.19$ and $g_{\perp} = 2.050$ characteristic of a $d_{x^2-y^2}$ ground-state matching either with a square planar, tetragonal distorted octahedral, or square pyramidal environment. The hyperfine coupling constant of the parallel component, A_{\parallel} , was 18.8 mT (Figure 4) compares well with the characteristics of $[\text{Cu}(\text{en})_2(\text{H}_2\text{O})_2]^{2+}$ elongated octahedral species (Supporting Information Table S4).^{40,41} This is consistent with two L_A ligands per Cu(II) ion in the solid material. Note that a material prepared with a L_A/Cu molar ratio of 1 instead of 2 exhibits two EPR signals consistent with a mixture of $[\text{Cu}(\text{L}_A)]^{2+}$ and $[\text{Cu}(\text{L}_A)_2]^{2+}$ inserted complexes. Though it appears that material DS-CuL_A contains a single copper(II) species, there are some slight differences with the genuine $[\text{Cu}(\text{L}_A)_2]^{2+}$ complex. The latter like $[\text{Cu}(\text{en})_2]^{2+}$ are characterized in solution by a slightly larger g_{\parallel}

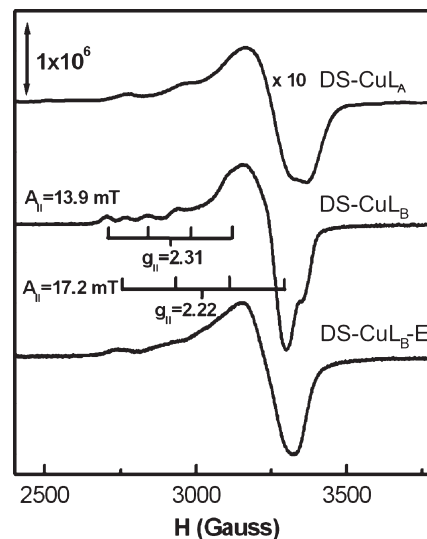


Figure 4. EPR of DS-CuL_A, DS-CuL_B, and DS-CuL_B-E. Experimental conditions: frequency = 9.35 GHz; power = 10 mW for DS-CuL_A and DS-CuL_B, 40 mW for DS-CuL_B-E; modulation amplitude = 1 G for DS-CuL_A, 6 G for DS-CuL_B, 9 G for DS-CuL_B-E, and modulation frequency = 100 kHz.

(=2.200) and a slightly smaller hyperfine value $A_{\parallel} = 18.8$ mT consistent with a weaker crystal field in the equatorial plan (x_y) than the solid inserted species. This indicates that the environment shifts either toward a square pyramidal symmetry expected with a strong ligand in the z axis or toward an elongated octahedral environment obtained with a pair of weak ligands in axial position. Since the siliceous matrix may provide either silanol or silanolate groups and since the former is close to water in the spectrochemical series, the most probable ligands here are the silanolate groups. The latter are σ and π donating group like OH^- and are weaker than H_2O .⁴² The g_{\perp} , less sensitive to any crystal field effect, is not commented here and is indeed nearly the same (~2.050) in solution and in the solid. These conclusions are consistent with an overall d-d bathochromic band shifting from 18000 cm^{-1} down to ca. 17000 cm^{-1} for complexes in solution to material inserted species.

The integrity of ligand L_B in the materials was monitored from the IR spectrum, looking at the band at 1623 cm^{-1} assigned to the stretching vibration, $\nu(\text{C}=\text{N})$, of the imino group (Scheme 1). Note that the ligand and metal-free DS-E material exhibits a small band at 1630 cm^{-1} (deformation, δ_{HOH}) reminiscent of H_2O traces. A slight shoulder at 1623 cm^{-1} could hardly be seen and precludes any definitive conclusion on the presence of the imine group in metal-free materials. Nonetheless, note that the $\nu(\text{C}=\text{N})$ band is expected to shift upward by about 20 cm^{-1} upon complexation as reported earlier.³⁶ The progressive increase in intensity and the shift of the band from 1630 up to 1650 cm^{-1} with higher metal loading in the DS-CuL_B series (M/Si = 0.5, 0.7, and 1.6 mol %) is consistent with the imino group being engaged in the copper complex (Supporting Information Figure S1). This band moves back down to 1630 cm^{-1} in material DS-CuL_B-H consistent with metal decomplexation and leaching after the acid treatment.

The UV-visible investigation reveals that the spectrum of DS-CuL_B, DS-CuL_B-E, and DS-CuL_B-H materials exhibit in all cases three main absorption bands below 300 nm, which can be attributed to $\pi-\pi^*$ transitions of the L_B ligand either free or complexed to the copper ion (Figure 5 and Supporting Information

(40) Lewis, W. B.; Alei, M.; Morgan, L. O. *J. Chem. Phys.* **1966**, *45*, 4003.

(41) Ganesan, R.; Viswanathan, B. *J. Phys. Chem. B* **2004**, *108*, 7102.

(42) Bonneviot, L.; Legendre, O.; Kermarec, M.; Olivier, D.; Che, M. *J. Colloid Interface Sci.* **1990**, *34*, 534–547.

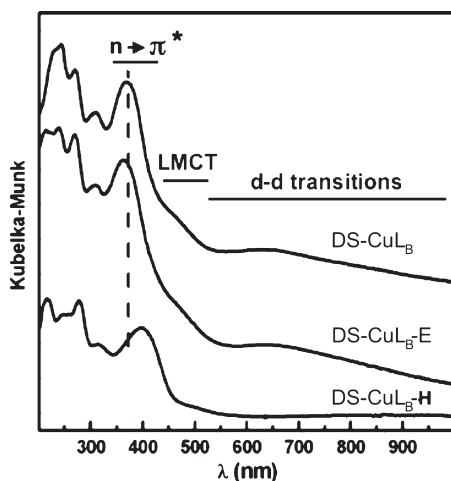


Figure 5. Solid-state UV–visible spectra of copper containing materials as synthesized, after template extraction, and after acid leaching test in materials **DS-CuL_B**, **DS-CuL_B-E**, and **DS-CuL_B-H**, respectively; the horizontal bars indicates the wavelength domains for the different electronic transitions in the inserted complex.

Table S3). These bands are also observed in the molecular analogues in solution (Supporting Information Figure S2). The complexation to copper affects only their relative intensity and is hardly exploitable per se. In the range 300–450 nm, two more bands are observed, also in the free ligand and in the complex. By contrast with the previous bands, their position depends on the solvent polarity and on the complexation to a metal ion. They are assigned to $n-\pi^*$ transitions of the imino group. The phenolic proton of the free neutral ligand in nonpolar solvents is located on the phenolic oxygen, giving rise to a band at ca. 330 nm. This band position is associated with the imino group with a free electron pair nonengaged in any sort of bonding. In polar solvents, the proton is transferred onto the nitrogen of the imino group, and the band undergoes a bathochromic shift down to ca. 400 nm reminiscent of the engagement of the electron pair in a bonding with the displaced proton.⁴³ In fact, both bands are often observed at the same time as a result of both proton locations being in equilibrium one with another. **HL_B** in ethanol exhibits two bands at 310 nm (strong) and 400 nm (weak) revealing the existence of an equilibrium in favor of the oxygen phenolic position. Inversely, the imino-nitrogen position, which generates a polar species, is the most favored situation in water, with a single band at 400 nm (Supporting Information Figure S2-A). In the presence of Cu(II) ions and in ethanol, the band position shifts to the intermediate position of 360 nm (Supporting Information Figure S2-B). In water, the bis hemisalen, **Cu(L_B)₂**, is in equilibrium with the monohemisalen complex, **Cu(L_B)(H₂O)₂**, as revealed by EPR (vide infra). As a consequence, some of the ligands **HL_B** are free in the water solution. The resulting band is broad and is consistent with a mixture of two bands at about 360 and 380 nm. Decreasing the pH from 11 down to 6 favors the shift of the band up to 380 nm, consistent with a complete leaching of the copper ion (**Cu-L_B-W11** to **W-6**, Supporting Information Figure S2-B). By comparison, in the absence of copper, the $n-\pi^*$ band of the free ligand **HL_B** does not shift in the pH range 6–11. For the solid **DS-3CuL_B**, there are also two bands observed at ca. 310 and 370 nm (Figure 5).

Upon careful extraction of the template, there is no change in the UV spectra (compare **DS-CuL_B** and **DS-CuL_B-E**). Upon

further acid treatment that yields metal leaching (**DS-CuL_B-H**), the low-energy band shifts from 370 nm down to 390 nm is consistent with a decomplexation of **L_B⁻**. It is worth noting that the presence of the peak at 310 nm in the spectrum of the starting material **DS-CuL_B** though rather weak is consistent with some noncomplexed **HL_B** ligands located in a nonpolar environment, i.e., more likely entrapped in the pore wall. Furthermore, an additional shoulder at ca. 470 nm was observed, which can be tentatively assigned to a ligand-to-metal charge transfer (LMCT) band.^{44–46} This band indeed disappears after metal extraction (Figure 5).

Finally, there is a weak and broad band centered at ca. 635 nm due to $d-d$ transitions of copper(II) ion. This band is lower in energy than the corresponding band of the **[Cu(L_B)₂]** molecular complex in ethanol (622 nm, Supporting Information Table S5), while the position is about the same in the spectrum of the aqueous solution of the complex (2 equiv **L_B⁻** versus Cu). This is consistent with a mixture of mono(salicylaldimine) copper(II) and bis(salicylaldimine) copper(II) complexes both in water and in the solid hybrid materials as already mentioned from the discussion of the $n-\pi^*$ band position.

The EPR spectrum of material **DS-CuL_B** (Figure 4) confirms the presence of two species: one with a g tensor mostly axial characterized by $g_{\parallel} = 2.31$, $A_{\parallel} = 13.9$ mT, and the other by $g_{\perp} = 2.22$, $A_{\perp} = 17.2$ mT. Both are consistent with a $d_{x^2-y^2}$ ground state and with an elongated octahedral environment, as above. The former is assigned to 1N3O environment in the equatorial plane around copper(II) ion and the latter with the 2N2O environment, consistent with one and two **L_B⁻** ligands per Cu(II) ion, respectively. Similar values have been reported by Murphy et al. for the same complexes grafted on nonmesostructured porous silica.²⁶ Indeed, such distribution in the solids is reminiscent of the equilibrium between mono- and bis-**L_B** complexes in water solution.^{47,48} This mixture of copper species in the **DS-3CuL_B** materials is in full agreement with the conclusion drawn from the UV–visible spectra and with the presence of some noncomplexed ligand **HL_B** entrapped in the pore wall.

4. Location of the Metal Complexes in the Solid Materials. All the above results allow us to confirm that the direct synthesis using **L_A** leads to inaccessible **[Ni(L_A)₂]²⁺** and **[Cu(L_A)₂]²⁺** complexes that are embedded in the pore walls and called as such in Scheme 2. The new spectroscopic characteristics of the incorporated complexes and the resulting inaccessibility are related to a direct coordination of the metal ions with silanolate moieties of the siliceous network. Note that the metal coordination is well-defined and can be exploited to tune the redox potential and/or the optical properties of the inorganic porous structure for bioinspired designed of catalysts.^{31–33} At the expense of the complex integrity, these complexes might be rendered accessible using calcination at high temperature as shown by Karakassides et al. for direct synthesis HSM or MCM materials containing copper(II) using also **L_A** ligand.^{11,12}

In material **DS-CuL_B-E**, two complexes are present, i.e., **[Cu(L_B)₂X₂]** and **[Cu(L_B)XL]** complexes ($X = \text{SiO}^-$ or OH^- and $L = \text{H}_2\text{O}$ or silanol ligands). Both are likely located in the wall according to the pore wall thickness and the high value of the pore volume. However, their weak resistance to the acid leaching test is

(44) Salavati-Niasari, M.; Mirsattari, S. N.; Bazarganipour, M. *Polyhedron* **2008**, *27*, 3653.

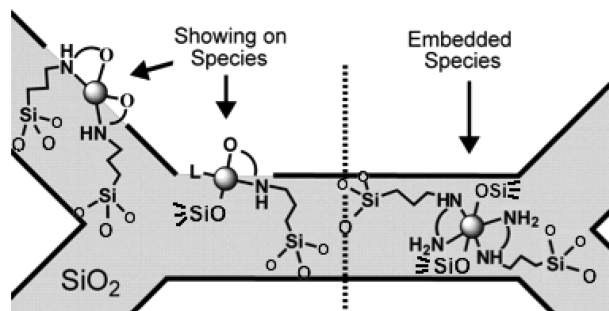
(45) Kurzak, K.; Kuzniarska-Biernacka, I.; Zurowska, B. *J. Sol. Chem.* **1999**, *28*, 133.

(46) Kuzniarska-Biernacka, I.; Kurzak, K.; Kurzak, B.; Jezierska, J. *J. Sol. Chem.* **2003**, *32*, 719.

(47) Baleizao, C.; Garcia, H. *Chem. Rev.* **2006**, *106*(9), 3987.

(43) Rospenk, M.; Krol-Starzomska, I.; Filarowski, A.; Koll, A. *Chem. Phys.* **2003**, *287*, 113.

Scheme 2. “Showing-On” and “Embedded” Framework Species in Materials DS-CuL_B-E and DS-NiL_B-E or DS-CuL_A-E, respectively^a



^a L is any neutral ligand such as water or silanol; for the sake of simplicity, the axial ligand are not represented for the “showing-on” species.

Table 2. Catalytic activity on phenol hydroxylation with H₂O₂ over various catalysts^a

material	phenol: H ₂ O ₂	phenol conv. (mol %)	diphenols selectivity (mol %)	CAT/ HQ
DS-E and DS-CuL _A -E	1:1	9	0	0
DS-CuL _B -E, 1st run	3:1	17	85	1.8
DS-CuL _B -E, 2nd run	3:1	15	84	1.9

^a Reaction conditions: solvent, buffer solution pH=6; phenol weight, 0.0989 g; phenol:Cu = 130:1; t = 2 h; T = 80 °C; [phenol] = 0.15 mol/L. After the first run, 80% of Cu(II) species remained in the catalysts (see text), and the catalyst mass was therefore corrected to afford the same phenol/Cu molar ratio.

reminiscent of their sensitivity to proton attack and their propensity to leach out Cu(II) ions. Then, it is proposed that both sites in DS-CuL_B-E are showing on the pore wall surface like outcrops and are called as such in Scheme 2. The rationale for such difference between L_A and L_B resides both in the more hydrophobic nature and in the neutrality of the complexes formed by the latter in comparison with the former. Both parameters are indeed strong driving forces to favor the location of the complexes in the organic side of the electrical palisade between the micelle and the aqueous solution during the initial steps of the silicate and organosilane moieties condensation. On the contrary, the ligand L_A favors direct binding of the metal to framework SiO⁻ anions leading to chemically inaccessible sites inside the pore wall.

5. Catalytic Activity of “Showing-On” Sites. To further probe the accessibility of the showing-on sites, the DS-CuL_B-E material was tested as heterogeneous catalyst for phenol hydroxylation using H₂O₂ as oxidant (Table 2). The reaction was performed at 80 °C and at pH=6 (buffer solution) using a phenol/Cu and a phenol/H₂O₂ molar ratio of 130:1 and 3:1, respectively. Note that no reaction takes place in these conditions without H₂O₂. Both metal-free DS-E and DS-CuL_A-E materials exhibited a conversion of ca. 9%, slightly higher than in the absence of any of both materials (~6–8%), but no selectivity toward catechol and hydroquinone was observed in all these cases. By contrast, DS-CuL_B-E was found active (17% conversion) in phenol hydroxylation, 85% of which was catechol (CAT) and hydroquinone (HQ) with a CAT/HQ ratio of 1.8. The remaining 15% of products corresponded to byproducts. By contrast, Ray et al. reported that the predominant product is the hydroquinone, while no benzoquinone was formed when bis(salicylaldimine) copper(II) complexes immobilized in the channel of MCM-41 are

used as catalyst. The characterization of this catalyst is poorly reported and does not allow clear comparison.⁴⁹ Other mesoporous materials with Cu(II) ions, such as Cu-SBA-15,⁵⁰ Cu-HMS,⁵¹ and Cu-exchanged Y zeolites,⁵² favor the formation of CAT, while TS-1 and Cu-CMM favor the formation of HQ. Despite the different local structure around copper, the catalytic activity of the showing-on sites does not differ much with previous zeolite or mesoporous silica-supported copper systems cited above.

After the first run, DS-CuL_B-E was recovered by filtration and then washed with ethanol and acetone and dried at 60 °C for 18 h. This so-obtained material was characterized by EPR spectroscopy. The copper EPR signal decreases by about 20%. This result suggested that the metal had partially leached out. In the second run, the reaction was run in the same conditions than for the first run, therefore with more catalysts to keep the phenol to copper ratio at 130. The rather identical activity and selectivity profiles shows that copper(II) is necessary to observe such performance. However, the loss of copper precludes any further conclusions on the real catalytic sites that could be either the inserted complex or the leached copper (ii) species. The equilibrium observed in solution for the molecular analogues was already an indication that L_B is a much weaker ligand than L_A and might be not the best candidate for catalytic applications. This may be the reason for the nonspecific difference between the present catalysts and the above cited systems where slight leaching may also occur.

Conclusions

Hybrid mesostructured porous materials containing Ni²⁺ or Cu²⁺ complexes with bidentate organosilane amino ligands in the framework have been synthesized. A direct synthesis has been optimized in order to condense the complex precursors with sodium silicate in aqueous solution, maintaining the structure integrity of both the porous material and the metal complex. The location of the complex in the direct synthesis material is controlled using two condensable organosilane ligands (Scheme 1): N-(2-aminoethyl)-3-aminopropyltrimethoxysilane, L_A, and, N-salicylaldimine-propylamine-trimethoxysilane, HL_B. The former ligand leads to inaccessible complexes with a coordination locked by two silanolate groups as exemplified in both DS-NiL_A and DS-CuL_A materials; they are named “embedded” sites. By contrast, L_B, which prevents direct bonding between the silanolate groups and the metal ion, yields accessible and catalytically active sites as shown in the DS-CuL_B material. These framework sites are named here “showing-on” (Scheme 2). By contrast with the post-grafted complexes, both embedded and showing-on complexes do not occupy the pore volume and do not affect the apparent pore wall thickness according to the nitrogen sorption investigations. Tuning independently both location and accessibility of the metal sites presents new opportunities to design multifunctional materials. For instance, inaccessible embedded sites may intervene as mere redox regulation centers, optical traps, or fluorescence centers while showing-on sites may be chosen for a specific catalytic activity and grafting of sites (metallic or organic) may be added to tune specific adsorption, acid–basic, or steric properties of the surface.

(49) Ray, S.; Mapolie, S. F.; Darkwa, J. *J. Mol. Catal. A: Chem.* **2007**, *267*, 143.

(50) Wang, L. P.; Kong, A. G.; Chen, B.; Ding, H. M.; Shan, Y. K.; He, M. Y. *J. Mol. Catal. A: Chem.* **2005**, *230*, 143.

(51) Fu, Z. H.; Chen, J. H.; Yin, D. L.; Yin, D. H.; Zhang, L. X.; Zhang, Y. Y. *Catal. Lett.* **2000**, *66*, 105.

(52) Wang, J.; Park, J. N.; Jeong, H. C.; Choi, K. S.; Wei, X. Y.; Hong, S. I.; Lee, C. W. *Energy Fuels* **2004**, *18*, 470.

(48) Zhou, W. J. Ph.D. Thesis, University of Lyon, France and East China Normal University, China, 2009.

Acknowledgment. Wen-Juan Zhou thanks the cooperative program between Ecole Normale Supérieure (ENS) de Lyon and East China Normal University (ECNU) in Shanghai, and thanks both French Government for the Eiffel Doctoral Scholarship and Chinese Government for Doctoral Scholarship to support her long stay in France.

Supporting Information Available: Figure S1 (FT-IR spectra of materials), Figure S2 (UV-visible spectra of L_B

and $Cu-L_B$ complexes in solution), Table S1 (metal content in mol % and molar ligand to metal ratio), Table S2 (yields on metal, ligand and silicon for the materials), Table S3 (IR and UV-visible data of the ligand and copper complexes), Table S4 (EPR characteristics of complexes in solution and in the materials), and Table S5 (IR and UV-visible data for the molecular ligand and metal complex analogues). This material is available free of charge via the Internet at <http://pubs.acs.org>.